Journal of Applied Electrochemistry **29**: 593–599, 1999.

4-Aminoantipyrine as an inhibitor of mild steel corrosion in HCl solution

S. S. ABD EL-REHIM*, MAGDY A. M. IBRAHIM and K. F. KHALED
Department of Chemistry, Faculty of Science, Ain Shams University, Cairo, Egypt
*(*author for correspondence)*

Received 9 June 1998; accepted in revised form 1 September 1998

Key words: 4-Aminoantipyrine, corrosion inhibition, hydrochloric acid solution, inhibitor, mild steel

Abstract

4-aminoantipyrine (AAP) was tested as a corrosion inhibitor for mild steel in 2 M HCl solution using different techniques: weight loss, potentiodynamic polarization and electrochemical impedance spectroscopy (EIS). The results showed that AAP is an inhibitor for mild steel in this medium. The inhibition was assumed to occur via adsorption of the inhibitor molecule on the metal surface. In the 20 to 60 °C temperature range, the AAP adsorption follows the Flory–Huggins isotherm and/or the El-Awady et al. kinetic-thermodynamic model. The protection efficiency increases with increasing inhibitor concentration (in the range 10^{-3}–10^{-2} M) but decreases with increasing temperature. The thermodynamic functions of dissolution and adsorption processes were calculated.

1. Introduction

Acid solutions are generally used for the removal of undesirable scale and rust in several industrial processes. Inhibitors are generally used in these processes to control the metal dissolution as well as acid consumption. Most of the well known acid inhibitors are organic compounds containing nitrogen, sulphur and/or oxygen atoms. Moreover, many *N*-heterocyclic compounds have been proved to be effective inhibitors for the corrosion of metals and alloys in aqueous media [1, 2]. The influence of organic compounds containing nitrogen on the corrosion of steel in acidic solutions has been investigated by several authors [2–8]. These organic compounds can adsorb on the metal surface, block the active sites on the surface and thereby reduce the corrosion rate.

This paper describes a study of the protection efficiency of 4-aminoantipyrine (AAP) for mild steel corrosion in acid medium. The behaviour of this compound in 2 M HCl has been investigated and its protection efficiency has been determined by chemical (weight loss) and electrochemical (potentiodynamic polarization and impedance) methods.

2. Experimental details

For the weight loss measurements, mild steel rods of chemical composition C 0.12%, Mn 0.85%, S 0.055%, P 0.05%, Si 0.09% and the remainder iron and of size 2 cm × 0.5 cm were used. The samples were polished with different grade emery papers up to 4/0 grade, cleaned with acetone, washed with doubly distilled water and finally dried. The cleaned samples were weighed before and after immersion in 2 M HCl for 2 h in the absence and presence of various concentrations of AAP and at different temperatures. The weight loss was expressed in g cm^{-2} h^{-1}.

For electrochemical measurements, the cell used was a conventional three electrodes Pyrex glass cell with a platinum counter electrode and a saturated calomel electrode (SCE) as reference. The working steel rod electrode was embedded in Araldite so that its cross sectional area (0.126 cm^2) was in contact with the solution. The potentiodynamic current–potential curves were recorded by changing the electrode potential automatically from −800 to 1000 mV with scan rate of 100 mV s^{-1}. EIS measurements were carried out in a frequency range of 10 kHz to 100 μHz using an amplitude of 5 mV peak to peak using a.c. signal at the open circuit potential (−500 mV). A potentiostat/galvanostat (EG&G model

273), frequency response analyser (model 5208) and a personal computer were used for electrochemical measurements. Impedence software from EG&G Princeton Applied Research was used for EIS measurements.

4-Aminoantipyrine (AAP) (F.W. 203) from Fluka and doubly distilled water were used for preparing fresh solutions. All solutions were deaerated for 10 min with nitrogen and experiments were carried out at constant temperature ± 0.5 °C. AAP has the following structure:

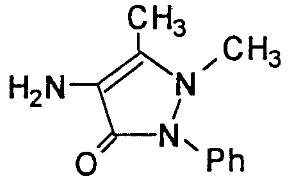

3. Results and discussion

The corrosion of mild steel in 2 M HCl in the absence and presence of various concentrations (10^{-3}–10^{-2} M) of AAP and at different temperatures (20–60 °C) was initially studied by weight loss experiments. The percentage protection efficiency (P) of AAP was calculated by applying the following relationship [9]:

$$P = \left(\frac{w_0 - w}{w_0}\right) \times 100 \tag{1}$$

where w_0 and w are the weight loss in the absence and presence of the inhibitor, respectively. Figure 1 shows the plot of the protection efficiency against the logarithmic concentration of AAP at different temperatures. Inspection of these data reveals that the presence of AAP in the solution inhibits the mild steel corrosion and the extent of protection efficiency increases with increasing inhibitor concentration. In contrast, the protection efficiency decreases with increasing temperature.

The curves of Figure 1 have the characteristic S-shaped isotherms indicative of an adsorption mechanism for the inhibition process. The studied inhibitor is a heterocyclic five membered ring with either half chair or envelope structure. The most important conformation being probably on symmetry C_2 (i.e., half chair) [10, 11]. The adsorption may be via the free amino group, which will cover by the rest of the inhibitor molecule acting as a hood [11]. The adsorption process involves the displacement of water molecules from the metal surface.

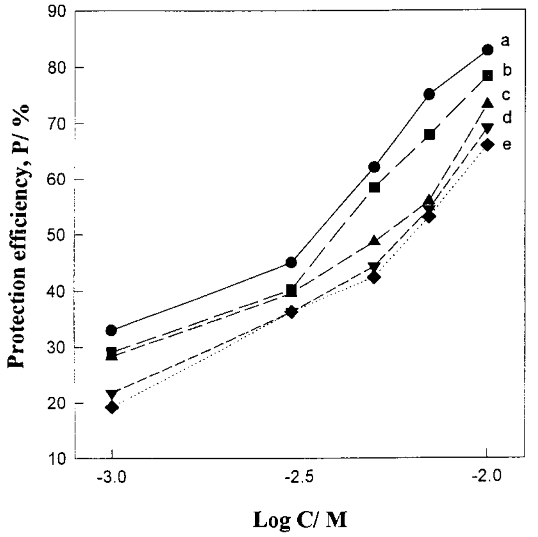

Fig. 1. Variation of the protection efficiency (P, %) with the logarithmic concentration of AAP for the mild steel in 2 M HCl at different temperatures: (a) 20, (b) 30, (c) 40, (d) 50 and (e) 60 °C.

Nine adsorption isotherms (Hill de Boer, Frumkin, Temkin, Langmuir, Parsons, Flory–Huggins, Dhar–Huggins, Bockris–Swinkels) [11] and El-Awady et al. [12, 13] were tested for their fit to the experimental data. The Flory–Huggins adsorption isotherm and the El-Awady et al. kinetic-thermodynamic model fit the experimental data well (correlation coefficient > 0.97). The adsorption isotherm relationships of Flory–Huggins and El Awady et al. are represented by Equations 2 and 3, respectively:

F.H.

$$\log(\theta/C) = \log xK + x\log(1-\theta) \tag{2}$$

E.A.

$$\log[\theta/(1-\theta)] = \log K' + y\log C \tag{3}$$

where θ is the degree of coverage $\{\theta = (w_0 - w)/w_0\}$; x is the number of active sites occupied by one inhibitor molecule or the number of water molecules replaced by one molecule of adsorbate. Values of x greater than one imply the formation of multilayers of the inhibitor on the metal surface. Values of x less than one, however, mean that a given inhibitor molecule will occupy more than one active site. The number of active sites of the surface occupied by one molecule of the inhibitor is given by the value of $(1/y)$. K is the binding constant of the adsorption reaction ($K = K'^{(1/y)}$) and C is the inhibitor concentration in the bulk of solution.

The binding constant of adsorption K is related to the standard free energy of adsorption $\Delta G^\circ_{\text{ads}}$ by the following equation:

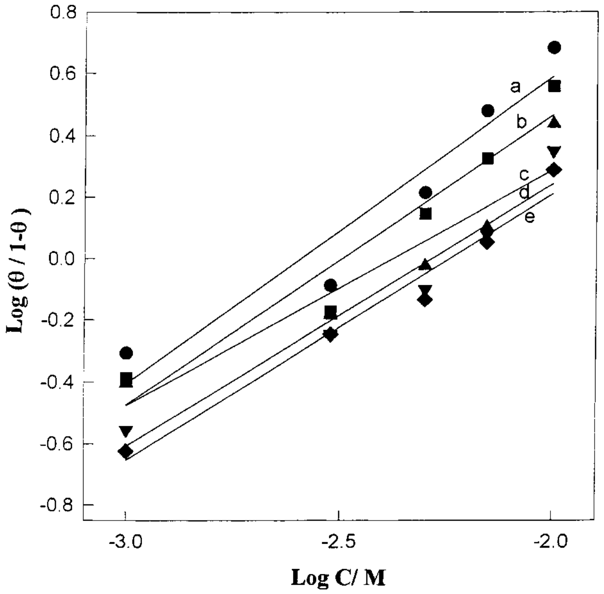

Fig. 2. Curve fitting of the corrosion data of mild steel in 2 M HCl in presence of AAP to the kinetic model at different temperatures: (a) 20, (b) 30, (c) 40, (d) 50 and (e) 60 °C.

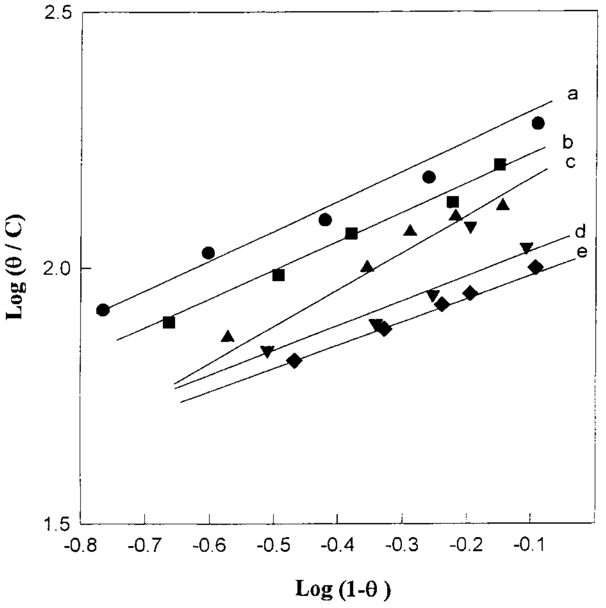

Fig. 3. Curve fitting of the corrosion data of mild steel in 2 M HCl in presence of AAP to Flory–Huggins isotherm at different temperatures: (a) 20, (b) 30, (c) 40, (d) 50 and (e) 60 °C.

$$K = \frac{1}{55.5} \exp\left(\frac{-\Delta G^{\circ}_{\mathrm{ads}}}{RT}\right) \tag{4}$$

where R is the universal gas constant and T is the absolute temperature. Application of the Flory–Huggins and El Awady models are illustrated in Figures 2 and 3, respectively. The calculated values of the binding constant K, free energy change $\Delta G^{\circ}_{\mathrm{ads}}$ and number of active sites x occupied by one inhibitor molecule are given in Table 1. The number of active sites x is approximately constant and equal to one under all conditions studied. This means that the inhibitor molecule adsorbs displacing one water molecule. The value of the constant K decreases with increasing temperature, indicating that the interactions between the adsorbed molecules and the metal surface are weakened and, consequently, the adsorbed molecules become easily removable. Such data explains the decrease in the protection efficiency with increasing temperature. Moreover, the values of $\Delta G^{\circ}_{\mathrm{ads}}$ are low, suggesting that the nature of the inhibitor adsorption is mainly physisorption [11, 15].

The average thermodynamic parameters $\Delta H^{\circ}_{\mathrm{ads}}$ and $\Delta S^{\circ}_{\mathrm{ads}}$ for the adsorption of AAP on mild steel in 2 M HCl in the 20–60 °C temperature range were calculated from the following equation [14]:

$$\log K = \frac{1}{2.303}\left(\frac{-\Delta H^{\circ}_{\mathrm{ads}}}{RT} + \frac{\Delta S^{\circ}_{\mathrm{ads}}}{R}\right) \tag{5}$$

where $\Delta H^{\circ}_{\mathrm{ads}}$ and $\Delta S^{\circ}_{\mathrm{ads}}$ are the enthalpy and entropy of the adsorption process, respectively. The calculated values for $\Delta H^{\circ}_{\mathrm{ads}}$ is $-36.8\ \mathrm{kJ\ mol^{-1}}$, $\Delta S^{\circ}_{\mathrm{ads}}$ is $-66.8\ \mathrm{J}\ K^{-1}\ \mathrm{mol^{-1}}$ and $\Delta G^{\circ}_{\mathrm{ads}}$ is $-18.5\ \mathrm{kJ\ mol^{-1}}$. The negative value of $\Delta H^{\circ}_{\mathrm{ads}}$ indicate that the adsorption of inhibitor molecules is an exothermic process [15]. The

Table 1. Inhibitor binding constant (K), free energy of adsorption ($\Delta G^{\circ}_{\mathrm{ads}}$), number of active sites (x) for AAP in 2 M HCl at different temperatures

Temp/K	Kinetic-thermodynamic model			Flory–Huggins isotherm		
	$1/y$	K	$\Delta G^{\circ}_{\mathrm{ads}}$ /kJ mol^{-1}	x	K	$\Delta G^{\circ}_{\mathrm{ads}}$/kJ mol^{-1}
293	1.0	391	–24.3	0.8	396	–24.4
303	1.1	310	–24.6	0.9	315	–24.6
313	1.3	241	–24.7	1.2	229	–24.6
323	1.1	191	–24.9	1.1	191	–24.9
333	1.2	176	–25.4	1.2	172	–25.4

magnitude of the values of ΔS°_{ads} and ΔH°_{ads} are characteristic of the occurrence of a replacement process during adsorption of inhibitor molecules on the metal surface [16].

The thermodynamic functions for the dissolution of mild steel in 2 M HCl in the absence and presence of various concentrations of AAP were obtained by applying the Arrhenius equation (Equation 6) and transition state equation (Equation 7), respectively:

$$\log(\text{Rate}) = -E^\circ_a/2.303\,RT + A \tag{6}$$

$$\text{Rate} = \frac{RT}{Nh}\exp\left(\frac{\Delta S^\circ}{R}\right)\exp\left(\frac{\Delta H^\circ}{RT}\right) \tag{7}$$

where E°_a is the apparent activation energy, ΔS° is the entropy of activation, ΔH° is the enthalpy of activation, h is Planck's constant and N is the Avogadro number. According to Equation 6 the apparent activation energy E°_a can be obtained by plotting log (rate) against $1/T$. Moreover, from Equation 7, a plot of $\log(\text{rate}/T)$ against $1/T$ should give straight line with a slope of $(-\Delta H^\circ/2.303\,R)$ and an intercept of $(\log R/Nh - \Delta S^\circ/2.303\,R)$. The calculated parameters are given in Table 2. Inspection of these data reveals that the apparent activation energy E°_a in HCl solution in the absence of AAP was 61.5 KJ mol^{-1}. The addition of AAP to the acid solution increases E°_a and the extent of the increase is proportional to the inhibitor concentration, indicating that the energy barrier for the corrosion reaction increases with AAP concentration. This means that the corrosion reaction will be further pushed to surface sites that are characterized by progressively higher values of E°_a as the concentration of the inhibitor in the acid solution becomes larger. The entropy of activation ΔS° in the absence and presence of AAP is large and negative. This implies that the activated complex in the rate determining step represents an association rather than a dissociation step, meaning that a decreases in disordering takes place on going from reactants to the activated complex [9, 10].

Table 2. Activation parameters of the dissolution of mild steel in 2 M HCl in the absence and presence of different concentrations of AAP

Concentration /M	E°_a /kJ mol^{-1}	ΔH° /kJ mol^{-1}	ΔS° /J K^{-1} mol^{-1}
0.000	61.5	58.8	−92.7
0.001	65.5	62.6	−82.9
0.003	66.6	64.0	−80.0
0.005	70.7	68.0	−69.1
0.007	74.7	72.0	−58.3
0.010	75.4	72.8	−59.1

Figure 4 shows typical anodic and cathodic potentiodynamic polarization curves for mild steel in 2 M HCl in the absence and presence of various concentrations

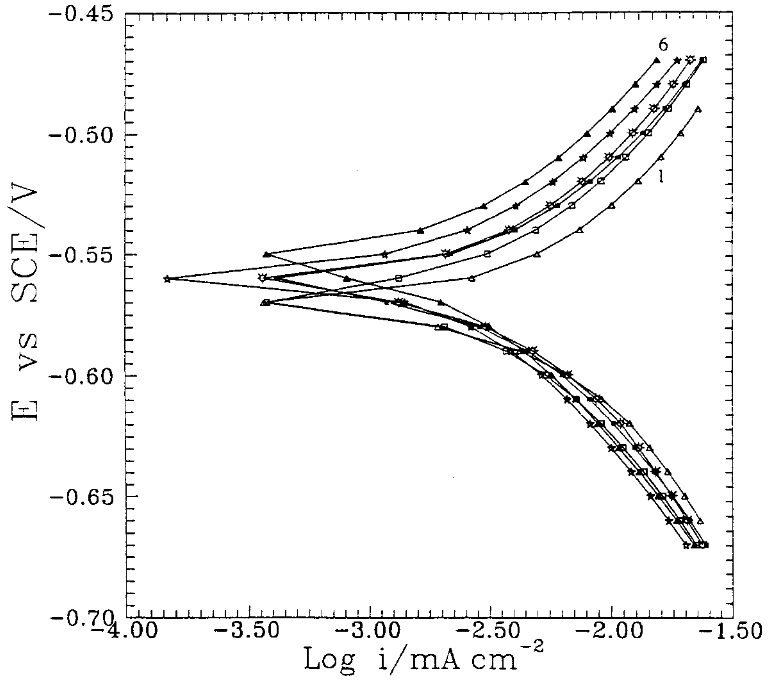

Fig. 4. Polarization curves of mild steel in 2 M HCl in presence of different concentrations of AAP: (1) 0.00, (2) 1 × 10^{-3}, (3) 3 × 10^{-3}, (4) 5 × 10^{-3}, (5) 7 × 10^{-3} and (6) 1 × 10^{-2} M.

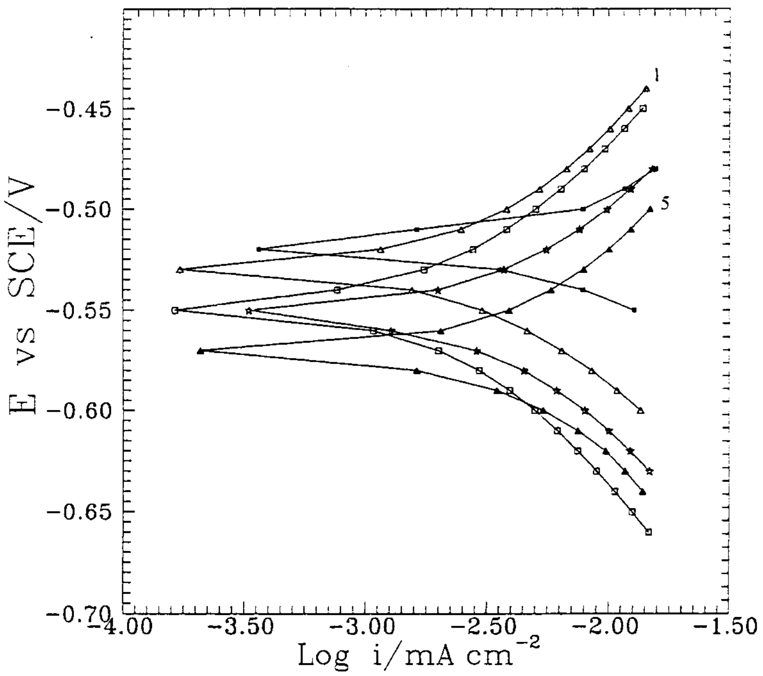

Fig. 5. Polarization curves of mild steel in 2 M HCl in presence of 0.003 M AAP at different temperatures: (1) 20, (2) 30, (3) 40, (4) 50 and (5) 60 °C.

(10^{-3}–10^{-2} M) of AAP at 30 °C. Figure 5 shows the effect of temperature on these polarization curves. These Figures show that the addition of AAP to the acid solution shifts the anodic polarization to more positive and the cathodic polarization to more negative values. The increase in AAP concentration increases the polarization shifts. The effect of AAP is more pronounced on anodic polarization than on cathodic polarization. Values of associated electrochemical parameters and the percentage protection efficiency (P) are given in Table 3. The protection efficiency is obtained from the following equation:

$$P = \left(\frac{i^{\circ}_{\mathrm{corr}} - i_{\mathrm{corr}}}{i^{\circ}_{\mathrm{corr}}}\right) \times 100 \qquad (8)$$

where $i_{\mathrm{corr}} = I_{\mathrm{corr}}/A$; A is the exposed surface area and $i^{\circ}_{\mathrm{corr}}$, i_{corr} are the uninhibited and inhibited corrosion current densities, respectively, determined by extrapolation of Tafel lines. The values of i_{corr} decrease with increasing AAP concentration but increase with increasing temperature. The decrease in i_{corr} with the inhibitor concentration is associated with a shift of corrosion potential E_{corr} to less negative values. These results suggest that AAP behaves mainly as an anodic inhibitor. The approximately constant values of the Tafel slopes (near to 0.12 V (decade)$^{-1}$ for b_c and 0.13 V (decade)$^{-1}$ for b_a) suggest that the inhibition mechanism for AAP involves a single reaction site blocking [18, 19]. Application of Equations 6 and 7 gave thermodynamic parameters for dissolution of mild steel in 2 M HCl in

Table 3. Electrochemical parameters for mild steel with AAP at 30 °C in 2 M HCl and (P, %) obtained from weight loss and potentiodynamic polarization tests

AAP conc. /M	$-E_{\mathrm{corr}}$ /V	I_{corr} /mA cm^{-2}	$-b_c$ /V (dec)$^{-1}$	b_a /V (dec)$^{-1}$	P Tafel data /%	P gravimetric data at 30 °C /%
0.000	0.555	3.79	0.150	0.169	–	–
0.001	0.548	2.64	0.187	0.148	30.3	33.0
0.003	0.547	2.09	0.126	0.149	44.7	45.0
0.005	0.544	1.49	0.114	0.125	60.6	62.1
0.007	0.540	1.22	0.113	0.126	67.7	75.0
0.010	0.538	1.04	0.112	0.121	72.6	82.8

Table 4. Activation parameters for the dissolution reaction of mild steel in the absence and in the presence of AAP on mild steel surface in HCl, calculated from potentiodynamic tests

$\Delta E°/\mathrm{kJ\,mol^{-1}}$	$\Delta H°/\mathrm{kJ\,mol^{-1}}$	$\Delta S°/\mathrm{J\,K^{-1}\,mol^{-1}}$
37.7	35.0	−121.6

the absence and presence of inhibitor and the results are given in Table 4. The activated parameters obtained from the potentiodynamic polarization method are lower than those obtained from the weight loss method.

Figure 6 shows the complex-plane impedance plots of mild steel in 2 M HCl without and with various concentrations of AAP (10^{-3}–10^{-2} M) at 30 °C. The equivalent circuit models used to fit the experimental results are given in Figure 7 as previously reported [20, 21]. The equivalent circuit model in Figure 7(a) can be given in a simplified equivalent circuit model as in Figure 7(b). The measured complex-plane impedance plot is similar to that calculated by the equivalent circuit model. The charge transfer resistance, R_{ct}, and the double layer capacitance, C_{dl}, were determined by analysis of the complex-plane impedance plots and their values are given in Table 5. It is clear that by increasing the AAP concentration R_{ct} are increased and C_{dl} values are decreased. The decrease in C_{dl} values with AAP concentration indicates an increase in the surface coverage of the inhibitor.

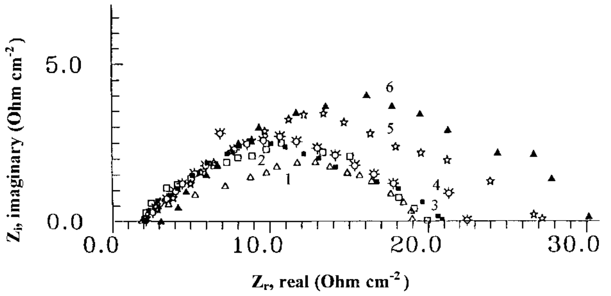

Fig. 6. Complex-plane impedance of mild steel in 2 M HCl in the presence of different concentrations of AAP at 30 °C: (1) 0.0, (2) 1 × 10^{-3}, (3) 3 × 10^{-3}, (4) 5 × 10^{-3} (5) 7 × 10^{-3} and (6) 1 × 10^{-2} M.

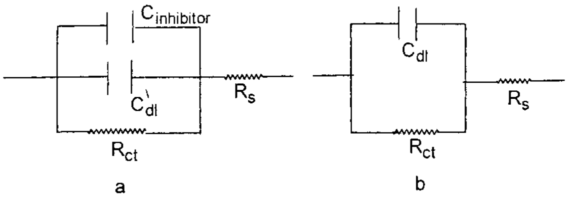

Fig. 7. Equivalent circuit model (a) can be given in a simplified equivalent circuit model (b). R_s and R_{ct} are solution and charge transfer resistance, respectively. $C_{inhibitor}$ is the capacitance of parts that the inhibitor is adsorbed. C'_{dl} is the capacitance of parts that the inhibitor is not adsorbed and C_{dl} is the apparent double layer capacitance.

Table 5. A.c. impedance data of steel in 2 M HCl solution containing different concentrations of AAP at 30 °C

Conc. /M	R_{ct} /Ω cm^{-2}	$1/R_{ct}$ Ω^{-1} cm^2	C_{dl} /μF	P /% (from EIS)
0.000	17.2	0.058	3683.6	–
0.001	19.1	0.052	1320.5	9.9
0.003	24.3	0.041	655.2	29.1
0.005	25.9	0.039	154.3	33.6
0.007	32.4	0.031	98.3	46.9
0.010	38.8	0.026	64.9	55.7

The corrosion current density I_{corr} was calculated using the charge transfer resistance, R_{ct} together with Stern–Geary equation [22]

$$I_{corr} = \frac{b_a b_c}{2.303\, R_{ct} A (b_a + b_c)} \tag{9}$$

where A is the electrode surface area and b_a and b_c are the Tafel slopes of the anodic and cathodic processes, respectively. The calculated values of I_{corr} are given in Table 5. It is seen that the values of I_{corr} decrease with increasing inhibitor concentration. The percentage protection efficiency, P, was calculated from the following equation:

$$P = \frac{(1/R_{ct})_0 - (1/R_{ct})}{(1/R_{ct})_0} \times 100 \tag{10}$$

where $(R_{ct})_0$ and (R_{ct}) are the uninhibited and inhibited charge transfer resistance, respectively. The calculated values of P are also included in Table 5. The values of I_{corr} and P obtained from EIS and potentiodynamic polarization measurements are in sequence.

The corrosion rates and the inhibition efficiencies obtained from the chemical method are somewhat different from those obtained from the electrochemical methods. The differences can be attributed to the fact that the weight loss method gives average corrosion rates, whereas electrochemical methods give instantaneous rates. These differences may also be expected to arise because of the difference in the time required to form an adsorbed inhibitor layer on the metal surface that is capable of corrosion inhibition [23].

4. Conclusions

The following can now be stated:

(i) 4-aminoantipyrine (AAP) behaves as an anodic inhibitor for mild steel corrosion in 2 M HCl.

(ii) The inhibition is due to the adsorption of the inhibitor molecules on the steel surface and blocking of active sites.
(iii) The protection efficiency increases with increase in inhibitor concentration but decreases with increase in temperature.
(iv) The data obtained fit both the Flory–Huggins isotherm and the El Awady thermodynamic-kinetic model very well.

References

1. A. El-Sayed, *J. Appl. Electrochem.* **27** (1997) 193.
2. G. Schmitt, *Br. Corros. J.* **19** (1984) 165.
3. J.M. Sykes, *Br. Corros. J.* **25** (1990) 175.
4. P. Chatterjee, M.K. Banerjee and K.P. Mukherjee, *Indian J. Technol.* **29** (1991) 191.
5. S. Rengamani, S. Muralidharan, M. Anbu Kulamdainathan and S. Venkatakrishna Iyer, *J. Appl. Electrochem.* **24** (1994) 355.
6. G.K. Gomma and M.H. Wahdan, *Bull. Chem. Soc. Jpn.* **67** (1994) 2621.
7. M. Ajmal, A.S. Mideen and M.A. Quraishi, *Corros. Sci.* **36** (1994) 79.
8. A. El-Sayed, *J. Appl. Electrochem.* **27** (1992) 193.
9. M.K. Gomma and M.H. Wahdan, *Mater. Chem. Phys.* **39** (1995) 209.
10. J. Marsh,'*Advanced Organic Chemistry*', 3rd edn. (Wiley Eastern, New Delhi 1988).
11. E. Khamis, A. Hosny and S. El-Hadary *Afinidad* (Rev. Quim. Teor. Aplic) **456** (1995) 95.
12. A. El-Awady, A. Abd El-Nabey, S. Aziz, M. Khalifa and H. Al-Ghamdey: *Int. J. Chem.* **1** (1990) 169.
13. A. El-Awady, A. Abd El-Nabey and S. Aziz, *J. Electrochem. Soc.* **139** (1992) 2149.
14. S. Sankarapapavinasam and M.F. Ahmed, *J. Appl. Electrochem.* **22** (1992) 390.
15. B.A. Abd El-Naby, E. Khamis, M.SH. Ramdan and A. El. Gindy. 8th European Symposium on Corrosion Inhibitors, Ann., Univ. Ferrara N. S., Sez. **10** (1995) 299.
16. M.J. Lampinen and M. Fomino, *J. Electrochem. Soc.* **140** (1993) 3537.
17. R.K. Dinnappa and S.M. Mayann, *J. Appl. Electrochem.* **11** (1981) 111.
18. G. Moretti, G. Quartarone, A. Tassan and A. Zingales, *Electrochim. Acta* **41** (1996) 1971.
19. T.P. Hoar and R.P. Khera, Proc. 1st European Symposium on Corrosion Inhibitors, Ferrara, Italy, University of Ferrara **73** (1960).
20. A. El-Sayed, *Corros. Prevention* & *Control.* **43** (1996) 29.
21. I. Sekine, M. Sabongi, H. Hagiuda, T. Oshibe, M. Yuasa, T. Imahama, Y. Shibata and T. Wake, *J. Electrochem. Soc.* **139** (1992) 3167.
22. A. El-Sayed, *J. Appl. Electrochem.* **27** (1997) 194.
23. S. Muraldharan, M. A. Quraishi and S.V.K. Iyer, *Corros. Sci.* **37**(11) (1995) 1739.